HHS Public Access

Author manuscript

J Neurosurg Spine. Author manuscript; available in PMC 2021 January 05.

Published in final edited form as:

J Neurosurg Spine. ; 31(4): 607–615. doi:10.3171/2019.4.SPINE19178.

Reduced field of view echo-planar imaging diffusion tensor MRI for pediatric spinal tumors

Lily H. Kim, BA[1], **Edward H. Lee, PhD**[2], **Michelle Galvez, MD**[3], **Murat Aksoy, PhD**[3], **Stefan Skare, PhD**[4], **Rafael O'Halloran, PhD**[5], **Michael S. B. Edwards, MD**[1], **Samantha J. Holdsworth, PhD**[6], **Kristen W. Yeom, MD**[3]

[1]Department of Neurosurgery, Stanford University School of Medicine, Stanford;

[2]Department of Electrical Engineering, Stanford University, Stanford, California;

[3]Department of Radiology, Stanford University School of Medicine, Stanford;

[4]Clinical Neuroscience, Karolinska Institute, Stockholm, Sweden;

[5]Hyperfine Research Inc., Guilford, Connecticut; University of Auckland, New Zealand

[6]Department of Anatomy and Medical Imaging & Centre for Brain Research, Faculty of Medical and Health Sciences, University of Auckland, New Zealand

Abstract

OBJECTIVE—Spine MRI is a diagnostic modality for evaluating pediatric CNS tumors. Applying diffusion-weighted MRI (DWI) or diffusion tensor imaging (DTI) to the spine poses challenges due to intrinsic spinal anatomy that exacerbates various image-related artifacts, such as signal dropouts or pileups, geometrical distortions, and incomplete fat suppression. The zonal oblique multislice (ZOOM)–echo-planar imaging (EPI) technique reduces geometric distortion and image blurring by reducing the field of view (FOV) without signal aliasing into the FOV. The authors hypothesized that the ZOOM-EPI method for spine DTI in concert with conventional spinal MRI is an efficient method for augmenting the evaluation of pediatric spinal tumors.

METHODS—Thirty-eight consecutive patients (mean age 8 years) who underwent ZOOM-EPI spine DTI for CNS tumor workup were retrospectively identified. Patients underwent conventional spine MRI and ZOOM-EPI DTI spine MRI. Two blinded radiologists independently reviewed two sets of randomized images: conventional spine MRI without ZOOM-EPI DTI, and conventional spine MRI with ZOOM-EPI DTI. For both image sets, the reviewers scored the findings based on lesion conspicuity and diagnostic confidence using a 5-point Likert scale. The reviewers also recorded presence of tumors. Quantitative apparent diffusion coefficient (ADC) measurements

Correspondence: Kristen W. Yeom: Lucile Packard Children's Hospital, Stanford University School of Medicine, Palo Alto, CA. kyeom@stanford.edu.

Author Contributions

Conception and design: Yeom, Edwards. Acquisition of data: Yeom, Galvez, Aksoy, Skare, O'Halloran, Edwards, Holdsworth. Analysis and interpretation of data: Yeom, Kim, Lee, Galvez, Aksoy, Skare, Holdsworth. Drafting the article: Kim. Critically revising the article: Yeom, Kim, Holdsworth. Reviewed submitted version of manuscript: all authors. Approved the final version of the manuscript on behalf of all authors: Yeom. Statistical analysis: Kim. Study supervision: Yeom.

Disclosures

Dr. Aksoy: direct stock ownership in HobbitView, Inc., and consultant for Ischemaview, Inc.

of various spinal tumors were extracted. Tractography was performed in a subset of patients undergoing presurgical evaluation.

RESULTS—Sixteen patients demonstrated spinal tumor lesions. The readers were in moderate agreement (kappa = 0.61, 95% CI 0.30–0.91). The mean scores for conventional MRI and combined conventional MRI and DTI were as follows, respectively: 3.0 and 4.0 for lesion conspicuity ($p = 0.0039$), and 2.8 and 3.9 for diagnostic confidence ($p < 0.001$). ZOOM-EPI DTI identified new lesions in 3 patients. In 3 patients, tractography used for neurosurgical planning showed characteristic fiber tract projections. The mean weighted ADCs of low- and high-grade tumors were 1201×10^{-6} and $865 \acute{} 10^{-6}$ mm^2/sec ($p = 0.002$), respectively; the mean minimum weighted ADCs were 823×10^{-6} and $474 \acute{} 10^{-6}$ mm^2/sec ($p = 0.0003$), respectively.

CONCLUSIONS—Diffusion MRI with ZOOM-EPI can improve the detection of spinal lesions while providing quantitative diffusion information that helps distinguish low- from high-grade tumors. By adding a 2-minute DTI scan, quantitative diffusion information and tract profiles can reliably be obtained and serve as a useful adjunct to presurgical planning for pediatric spinal tumors.

Keywords

diffusion tensor imaging; central nervous system tumors; echo-planar imaging; spine imaging; pediatric neurosurgery; ZOOM-EPI; diffusion MRI; oncology

RESECTION increases the likelihood of long-term patient survival for many types of spinal tumors.[11,26] With the advances in microsurgical techniques, aggressive resection has become increasingly feasible,[9] but methods that optimize lesion characterization and delineation prior to spinal surgery could further contribute to favorable surgical outcome.[3,29] At present, MRI is the main diagnostic imaging modality for neurosurgical evaluation of spinal lesions.[1,30] For lesion characterization, advanced MRI methods, such as diffusion-weighted imaging (DWI) and diffusion tensor imaging (DTI), have been shown to help characterize spinal neoplasms, such as intramedullary tumors,[29] gliomas,[18] cord lesions,[36] and vertebral body metastases.[7,21]

Unlike more global applications of diffusion MRI for brain evaluation,[20,41] routine clinical application of spinal DWI is often hampered by artifacts exacerbated by intrinsic spinal anatomy.[5] Single-shot echo-planar imaging (EPI), a particular type of pulse sequence widely used to perform DWI,[43] is suboptimal for spine imaging, as it is highly sensitive to off-resonance artifacts created by the magnetic field inhomogeneity surrounding the spinal columns and the cord.[27] These artifacts are exacerbated by small voxel sizes required to depict the small cross-sectional area of the spinal cord, and a large field of view (FOV) required to avoid aliasing of tissues outside the FOV.[5] Other anatomical characteristics unique to spine, such as the proximity to air cavities in the thoracic spine, nonuniform bone density of the vertebrae, and motion from cardiac or respiratory activity, also pose technical challenges that result in signal dropout/pile-ups, geometrical distortions, and incomplete fat suppression.[3,10,27,28]

Despite these hurdles, DWI in the spine could offer valuable information.[5] DWI, which uses image contrast based on diffusivity of water molecules, and DTI, which allows for analysis

of the 3D shape of the diffusion ("diffusion tensor"), uniquely offer quantitative data on tissue microstructure, benefits not offered by other MRI sequences.[14] Various diffusion-weighted MRI techniques have been developed to address current technical limitations. One such method is the zonal oblique multislice (ZOOM)–EPI technique, which is better suited for the narrow and longitudinal spine anatomy, as it uses reduced (rectangular) FOV without aliasing, thereby allowing for reduced image blurring and geometrical distortion.[19,33,37–39]

Although the ZOOM-EPI technique has been used to image CNS structures,[2,10,13,24,37,38] its clinical application for evaluating spinal neoplasms, especially in the pediatric population, is lacking. Here, we share our institutional experience of applying ZOOM-EPI DTI in patients undergoing diagnostic workup for potential spinal tumors. We hypothesized that ZOOM-EPI DTI can augment evaluation of pediatric spinal neoplasms by improving lesion detection and provide information on tumor and adjacent tissue characteristics that could enhance presurgical evaluation.

Methods

Patient Population

We retrospectively identified 38 consecutive patients who underwent ZOOM-EPI spine DTI for CNS tumor workup at our institution. All were pediatric patients except one adult patient who was seen by a pediatric neurosurgeon and treated at our children's hospital for her spinal tumor (pilocytic astrocytoma). The study was conducted after we received approval from our institutional review board. Consent from the patients' parents, or the patients when appropriate, was obtained prior to image acquisition.

Image Acquisition

All patients underwent both conventional (e.g., T2-weighted and T1-weighted with contrast) MRI sequences as well as spine ZOOM-EPI DTI imaging with a 1.5T or 3T magnet (GE Medical Systems) using a 4-channel spinal coil. In patients 7 years or younger, imaging was performed under monitored sedation.

ZOOM-EPI DTI

The ZOOM-EPI DTI parameters were as follows: TR 3 seconds, 7 slices with 3-mm thickness and no gap, zoom-angle $\theta = 10°$, TE 73 msec, partial Fourier encoding, 5 $b = 0$, 35 isotropically distributed diffusion-weighted directions with $b = 500$ sec/mm^2, and a scan time of 2 minutes. The basic principle of the ZOOM-EPI technique is described extensively elsewhere.[19,33,37,38] Briefly, ZOOM-EPI is a multislice technique, which reduces the FOV in the phase-encoding direction, by applying a 90° slice selective pulse, followed by a tilted 180° refocusing pulse. The resulting parallelogram-shaped inner volume area is depicted in Fig. 1. The resultant smaller FOV allows for a higher resolution when the matrix size is held the same, while the shorter length of the EPI echo train minimizes susceptibility-induced geometrical distortion (Fig. 2). The shorter EPI echo train decreases distortion by minimizing the length of time that spins undergo dephasing arising from distortions in the local field.[35]

Postprocessing

Postprocessing was performed in select ZOOM-EPI images by correcting for distortion with a displacement field calculated from positive and negative distortion images. An example is shown in Fig. 3.

Image Evaluation

Two blinded, board-certified radiologists (K.W.Y., M.G.) independently reviewed and compared conventional spine MR images alone versus conventional MR images combined with ZOOM-EPI DTI scans, which were assigned in a random manner. In detail, first, the conventional spine MRI sequences were isolated, randomized, and presented for the radiologist for a blinded review, including lesion identification and Likert scoring. Next, for the same study cohort, the conventional MRI sequences combined with the ZOOM-EPI DTI were randomized and presented to the same radiologists for lesion detection and Likert scoring. A flowchart illustrating image acquisition and the evaluation process is available in Fig. 4.

The reviewers scored the scans for lesion conspicuity and diagnostic confidence using a 5-point Likert scale.[42] This scale has been widely used in the radiology literature to evaluate and compare the quality of different imaging techniques.[45] The degree of contrast between the lesion and the background was assessed for lesion conspicuity. Diagnostic confidence was based on the final diagnosis, including surgical pathology, and the image quality that enabled lesion detection. The 5-point Likert score ranged from 1 to 5, with “1” corresponding to least conspicuous (when evaluating lesion conspicuity) or least confident (when evaluating diagnostic confidence) and “5” referring to most conspicuous (when evaluating lesion conspicuity) or most confident (when evaluating diagnostic confidence).

Apparent Diffusion Coefficient Evaluation

The spine MRI scans in the data set were randomized, and, by consensus review, the reviewers performed region of interest (ROI) analysis of the spinal tumors on all slices and over the entire boundary of the tumor, blinded to the final pathology. The mean and minimum apparent diffusion coefficient (ADC) values were obtained within this ROI in all available axial planes of the tumor and then averaged over each slice.

DTI Tractography

In select presurgical cases (spinal cord ganglioglioma, pilocytic astrocytoma, and infiltrating glioma), tractography was performed for potential application for neurosurgical planning. For each data set, fiber tractography was performed using custom-built software. Seed regions were placed within the brainstem or the spinal cord, including the tumor and surrounding tissue. Euler’s method[44] was used for tracking, with a fractional anisotropy (FA) threshold of 0.15 and curvature threshold of 40°.

Statistical Analysis

The kappa score was used to quantify the degree of interrater agreement with a corresponding confidence interval. Likert scale scores for conventional MRI versus

conventional MRI combined with ZOOM-EPI DTI were assessed with a linear regression model adjusting for age, and the STATA "margins" command was used to estimate the means. We calculated the weighted average of mean ADC values, with the respective area of the ROI serving as weights. The one-way ANOVA test was used to compare the weighted average of mean ADC values between low- and high-grade tumors. A p value < 0.05 was considered statistically significant. All analyses were performed using STATA version 11 (StataCorp.).

Results

Study Cohort

Of 38 patients (mean age 8 years; 12 females and 26 males), 16 had spinal lesions. The types of spinal lesions included medulloblastoma drop metastasis, intramedullary ependymoma seeded from a posterior fossa mass, brainstem/cervical ganglioglioma, brainstem and cervical cord pilocytic astrocytoma, schwannoma (associated with neurofibromatosis types I and II), spinal neuroblastoma, pineoblastoma, and thoracic cord primitive neuroectodermal tumor. Despite variable spinal anatomy, alignment, and curvature/scoliosis related to underlying spinal tumor, the diagnostic quality of DTI was achievable using the ZOOM-EPI method. Tractography in select cases showed feasibility of tract profile generation using ZOOM-EPI DTI (see case 2 below and Fig. 7). Detailed demographic and clinical information is summarized in Table 1.

Reviewer Agreement

After adjusting for age, the estimated mean Likert scale score for lesion conspicuity was 4.0 (SE 0.12) for combined conventional MRI and DTI, which was significantly higher than the estimated mean score of 3.0 (SE 0.12) for conventional MRI alone (p = 0.0039). The mean Likert scale score for diagnostic confidence was also significantly higher for combined conventional MRI and DTI than that for conventional MRI only (2.8 vs 3.9, p < 0.001) (Fig. 5). The kappa score was 0.61 (95% CI 0.30–0.91), indicating moderate agreement among the reviewing radiologists.

ADC Measurements

The average weighted mean ADC values for low-grade tumors and high-grade tumors were 1202×10^{-6} mm^2/sec and 865×10^{-6} mm^2/sec, respectively. The difference was statistically significant (p = 0.002). The average weighted minimum ADC values were 823×10^{-6} mm^2/sec for low-grade tumors and 474×10^{-6} mm^2/sec for high-grade tumors (p = 0.0003).

Case Illustrations

Case 1—The ZOOM-EPI $b = 0$ sec/mm^2, isotropic DWI, color FA, and tractography images were obtained in a 6-year-old girl with pilocytic astrocytoma in the brainstem (Fig. 6). The patient had a well-encapsulated tumor, which was surgically found to lack local tumor infiltration and was confirmed pathologically as a low-grade tumor (grade I pilocytic astrocytoma).

Case 2—Figure 7 shows ZOOM-EPI $b = 0$ sec/mm^2, isotropic DWI, color FA, and tractography images obtained in a 5-year-old boy with a suspected thoracic cord neoplasm. ZOOM-EPI DTI data sets were acquired at 1.5T, FOV 18 cm ´ 4.5 cm, and matrix size 192 ´ 48. The patient had an aggressive neoplasm with an infiltrative tumor biology where neoplastic cells infiltrated and traversed alongside the spinal tracts. At surgery, the lesion was adherent and difficult to completely excise due to its infiltrative nature. Pathologic assessment revealed infiltrating grade II astrocytoma, confirming preoperative diagnostic suspicion based on ZOOM-EPI data.

Discussion

Here, we report the clinical application of ZOOM-EPI DTI in evaluating pediatric spinal tumors. Compared with the diagnostic evaluation using conventional spine MRI alone, the addition of a 2-minute ZOOM-EPI DTI resulted in higher scoring by 2 independent radiologists, for both lesion conspicuity and diagnostic confidence. Our pilot study results suggest that ZOOM-EPI DTI could provide insight into tumor grade, improve lesion detection, and, through tract profile generation, provide a mechanism for delineating tumor boundaries and adjacent traversing white matter trajectories.

Tumors of the CNS constitute the most common type of malignancies in children, but less than 10% of pediatric CNS tumors involve the spine.[23] Although less common than brain tumors, pediatric spinal tumors still carry considerable morbidity and mortality burdens, with their insidious nature often delaying diagnosis in children.[15,25] Spinal tumors may involve the spinal column or spinal cord, which can be further classified as intramedullary if they originate from spinal cord itself or extramedullary if they arise from structures surrounding the cord, such as the membrane or nerve roots.[1] For both types of spinal tumors, resection, when feasible, provides symptomatic relief from cord compression and increases the chance of long-term survival.[12,26,31] In addition to therapeutic resection, surgery often serves as the first diagnostic step for tumor histology.[8]

Optimizing methods for spinal tumor visualization is an important task for neurosurgical planning. MRI currently serves as the current standard-of-care diagnostic modality for detecting spinal lesions.[1] In addition to conventional MRI such as T2-weighted imaging, conventional 3-direction DWI can further characterize cord lesions, such as ischemia, infectious or toxic-metabolic process, and dermoid/epidermoid.[5,20] Taken one step further, DTI with its multiple additional diffusion directions could further probe spinal tract projections and potentially aid surgical navigation.[8,22]

However, due to the large off-resonance effects and geometric distortion that arise with conventional single-shot EPI DTI, the application of diffusion-weighted MRI in the spine poses many technical challenges. Multishot EPI methods exist to help mitigate susceptibility-related artifacts; however, the resulting phase errors that can occur between EPI shots can result in ghosting artifacts. These difficulties can result in artifact-laden, low-signal images of the spinal cord, which are often suboptimal for diagnostic evaluation. Cardiac gating (usually through finger pulse oximeter) can mitigate some motion-related artifacts in multishot EPI, but pulsatile cord motion or small patient motion can still plague

image quality.[32] Pseudo-lesions created by CSF flow artifacts may even obscure underlying lesions.[6]

Pediatric spine imaging can pose additional challenges due to the small cord size (limiting the signal-to-noise ratio) and prominent vasculature in young children[34] that can masquerade as lesions or create flow-related artifacts. Furthermore, long scan times that are sometimes used for higher-quality DTI in brain applications may be clinically impractical in children who might be motion-prone.

The ZOOM-EPI DTI technique addresses some of these challenges by using a tilted refocusing pulse to reduce the phase-encoding FOV (and thereby reducing geometrical distortion and image blurring) without giving rise to confounding aliasing. The reduced FOV is better suited for the long, narrow anatomy of the spine and its small cross-sectional size,[16,40] and enables a higher resolution for a fixed matrix size. Although this study was restricted to application of the ZOOM-EPI technique to the preoperative, diagnostic step of tumor evaluation, the reduced distortion may be useful in the intraoperative and postoperative stages as well, in the setting of air and blood products.

Prior studies have examined the ZOOM-EPI technique on adult volunteers with normal spinal cord,[2,13] imaging of small structures such as the optic nerve,[38] or its potential role for identifying pathologic changes of the hippocampus in adults with temporal lobe epilepsy.[24] No prior study has applied the ZOOM-EPI method for DTI for pediatric spine imaging or assessed its potential role for interrogating spinal pathology. In our study, the addition of ZOOM-EPI DTI to routine clinical spine MRI comprising conventional T2- and T1-weighted postcontrast sequences improved radiologist scores for diagnostic confidence and lesion conspicuity and suggests that ZOOM-EPI DTI could be a useful adjunct, particularly with its relatively efficient scan time of 2 minutes for a sagittal spine signal acquisition. This scan time efficiency renders it particularly favorable when acquiring images in young children or those at higher risk of patient motion.[17]

Despite its potential for clinical application, there are pitfalls for the ZOOM-EPI method for spinal DTI. As with all imaging, ZOOM-EPI DTI is susceptible to motion.[4] But, given its scan time efficiency, risk of motion is lower than that for conventional DTI sequences with longer scan times. The multislice capability of ZOOM-EPI may be called into question, given that the tilted-slice approach may saturate neighboring slices, thereby reducing the signal-to-noise ratio. However, since the useful anatomical region typically resides in the center of the slice, our experience suggests that it is possible to obtain high-quality scans with small zoom angles (10°) to reduce saturation effects.

A limitation of our study is its retrospective nature. Our study population is also relatively small, although it is comparable to or larger than those of previous studies on this technique.[10,13] The difficulty of obtaining a larger study sample also reflects the rarity of spinal tumors in children.[1] While we demonstrated the utility of this technique in a small subset of neurosurgical patients with spinal tumors, we suggest that further studies explore its use in other nonneoplastic conditions of the spine in which the value of DTI has been implicated, such as spinal trauma and infection.[28] Furthermore, because only patients with

suspected spinal lesions were imaged with the ZOOM-EPI DTI technique at our institution, we were unable to compare its utility with that of conventional MRI alone in a large group of healthy controls. Our results are based on single-institution experience, which calls for future work that encompasses MRI equipment from different vendors in a multicenter study.

Conclusions

We demonstrated that spinal DTI can be useful for the tumor workup of pediatric spinal neoplasms in clinical settings and that ZOOM-EPI is a useful acquisition method to maintain distortions within a reasonable limit. The addition of a ZOOM-EPI DTI sequence to conventional spinal MRI enhanced diagnostic evaluation for pathologic tumor grade and further defined the relationship between spinal tracts and the underlying lesion. Its efficient scan time (2 minutes) suggests its feasibility for incorporating into neurosurgical and radiology practices that see large clinical volumes.

Acknowledgments

This work was supported in part by the NIH (grant nos. 5R01EB002711, 5R01EB008706, 3R01EB008706, 5R01EB006526, 5R21EB006860, 2P41RR009784, and 1R21HD08380301A1), the Center of Advanced MR Technology at Stanford (P41RR09784), the Lucas Foundation, and the Swedish Research Council (K2007-53P-20322-01-4).

ABBREVIATIONS

ADC	apparent diffusion coefficient
DTI	diffusion tensor imaging
DWI	diffusion-weighted imaging
EPI	echo-planar imaging
FA	fractional anisotropy
FOV	field of view
ROI	region of interest
ZOOM	zonal oblique multislice

References

1. Abul-Kasim K, Thurnher MM, McKeever P, Sundgren PC: Intradural spinal tumors: current classification and MRI features. Neuroradiology 50:301–314, 2008 [PubMed: 18084751]
2. Alizadeh M, Poplawski MM, Fisher J, Gorniak RJT, Dresner A, Mohamed FB, et al. : Zonally magnified oblique multislice and non-zonally magnified oblique multislice DWI of the cervical spinal cord. AJNR Am J Neuroradiol 39:1555–1561, 2018 [PubMed: 29903926]
3. Andre JB, Bammer R: Advanced diffusion-weighted magnetic resonance imaging techniques of the human spinal cord. Top Magn Reson Imaging 21:367–378, 2010 [PubMed: 22158130]
4. Atkinson D, Porter DA, Hill DL, Calamante F, Connelly A: Sampling and reconstruction effects due to motion in diffusion-weighted interleaved echo planar imaging. Magn Reson Med 44:101–109, 2000 [PubMed: 10893527]

5. Bammer R, Fazekas F: Diffusion imaging of the human spinal cord and the vertebral column. Top Magn Reson Imaging 14:461–476, 2003 [PubMed: 14872166]
6. Barakat N, Mohamed FB, Hunter LN, Shah P, Faro SH, Samdani AF, et al. : Diffusion tensor imaging of the normal pediatric spinal cord using an inner field of view echo-planar imaging sequence. AJNR Am J Neuroradiol 33:1127–1133, 2012 [PubMed: 22300927]
7. Byun WM, Shin SO, Chang Y, Lee SJ, Finsterbusch J, Frahm J: Diffusion-weighted MR imaging of metastatic disease of the spine: assessment of response to therapy. AJNR Am J Neuroradiol 23:906–912, 2002 [PubMed: 12063214]
8. Choudhri AF, Whitehead MT, Klimo P Jr, Montgomery BK, Boop FA: Diffusion tensor imaging to guide surgical planning in intramedullary spinal cord tumors in children. Neuroradiology 56:169–174, 2014 [PubMed: 24395215]
9. Constantini S, Miller DC, Allen JC, Rorke LB, Freed D, Epstein FJ: Radical excision of intramedullary spinal cord tumors: surgical morbidity and long-term follow-up evaluation in 164 children and young adults. J Neurosurg 93 (2 Suppl):183–193, 2000
10. Dowell NG, Jenkins TM, Ciccarelli O, Miller DH, Wheeler-Kingshott CA: Contiguous-slice zonally oblique multislice (CO-ZOOM) diffusion tensor imaging: examples of in vivo spinal cord and optic nerve applications. J Magn Reson Imaging 29:454–460, 2009 [PubMed: 19161202]
11. Fehlings MG, Mercier D: Factors predicting the resectability of intramedullary spinal cord tumors and the progression-free survival following microsurgical treatment. J Neurosurg Spine 11:588–590, 2009 [PubMed: 19929362]
12. Gilard V, Goia A, Ferracci FX, Marguet F, Magne N, Langlois O, et al. : Spinal meningioma and factors predictive of post-operative deterioration. J Neurooncol 140:49–54, 2018 [PubMed: 29926318]
13. Grussu F, Schneider T, Zhang H, Alexander DC, Wheeler-Kingshott CA: Neurite orientation dispersion and density imaging of the healthy cervical spinal cord in vivo. Neuroimage 111:590–601, 2015 [PubMed: 25652391]
14. Huisman TA: Diffusion-weighted and diffusion tensor imaging of the brain, made easy. Cancer Imaging 10 (Spec No A):S163–S171, 2010 [PubMed: 20880787]
15. Huisman TA: Pediatric tumors of the spine. Cancer Imaging 9 (Spec No A):S45–S48, 2009 [PubMed: 19965293]
16. Jeong EK, Kim SE, Guo J, Kholmovski EG, Parker DL: High-resolution DTI with 2D interleaved multislice reduced FOV single-shot diffusion-weighted EPI (2D ss-rFOV-DWEPI). Magn Reson Med 54:1575–1579, 2005 [PubMed: 16254946]
17. Leemans A, Jones DK: The B-matrix must be rotated when correcting for subject motion in DTI data. Magn Reson Med 61:1336–1349, 2009 [PubMed: 19319973]
18. Maesawa S, Fujii M, Nakahara N, Watanabe T, Wakabayashi T, Yoshida J: Intraoperative tractography and motor evoked potential (MEP) monitoring in surgery for gliomas around the corticospinal tract. World Neurosurg 74:153–161, 2010 [PubMed: 21300007]
19. Mansfield P, Ordidge RJ, Coxon R: Zonally magnified EPI in real time by NMR. J Phys E Sci Instrum 21:275–280, 1988
20. Mascalchi M, Filippi M, Floris R, Fonda C, Gasparotti R, Villari N: Diffusion-weighted MR of the brain: methodology and clinical application. Radiol Med (Torino) 109:155–197, 2005 [PubMed: 15775887]
21. Messiou C, Collins DJ, Giles S, de Bono JS, Bianchini D, de Souza NM: Assessing response in bone metastases in prostate cancer with diffusion weighted MRI. Eur Radiol 21:2169–2177, 2011 [PubMed: 21710270]
22. Pujol S, Wells W, Pierpaoli C, Brun C, Gee J, Cheng G, et al. : The DTI challenge: toward standardized evaluation of diffusion tensor imaging tractography for neurosurgery. J Neuroimaging 25:875–882, 2015 [PubMed: 26259925]
23. Rickert CH, Paulus W: Epidemiology of central nervous system tumors in childhood and adolescence based on the new WHO classification. Childs Nerv Syst 17:503–511, 2001 [PubMed: 11585322]

24. Salmenpera TM, Simister RJ, Bartlett P, Symms MR, Boulby PA, Free SL, et al. : High-resolution diffusion tensor imaging of the hippocampus in temporal lobe epilepsy. Epilepsy Res 71:102–106, 2006 [PubMed: 16870399]
25. Samartzis D, Gillis CC, Shih P, O'Toole JE, Fessler RG: Intramedullary spinal cord tumors: part I—epidemiology, pathophysiology, and diagnosis. Global Spine J 5:425–435, 2015 [PubMed: 26430598]
26. Samuel N, Tetreault L, Santaguida C, Nater A, Moayeri N, Massicotte EM, et al. : Clinical and pathological outcomes after resection of intramedullary spinal cord tumors: a single-institution case series. Neurosurg Focus 41(2):E8, 2016
27. Saritas EU, Cunningham CH, Lee JH, Han ET, Nishimura DG: DWI of the spinal cord with reduced FOV single-shot EPI. Magn Reson Med 60:468–473, 2008 [PubMed: 18666126]
28. Sąsiadek MJ, Szewczyk P, Bladowska J: Application of diffusion tensor imaging (DTI) in pathological changes of the spinal cord. Med Sci Monit 18:RA73–RA79, 2012 [PubMed: 22648262]
29. Setzer M, Murtagh RD, Murtagh FR, Eleraky M, Jain S, Marquardt G, et al. : Diffusion tensor imaging tractography in patients with intramedullary tumors: comparison with intra-operative findings and value for prediction of tumor resect-ability. J Neurosurg Spine 13:371–380, 2010 [PubMed: 20809733]
30. Shibahara I, Saito R, Osada Y, Kanamori M, Sonoda Y, Kumabe T, et al. : Incidence of initial spinal metastasis in glioblastoma patients and the importance of spinal screening using MRI. J Neurooncol 141:337–345, 2019 [PubMed: 30414100]
31. Sofuoğlu OE, Abdallah A: Pediatric spinal ependymomas. Med Sci Monit 24:7072–7089, 2018 [PubMed: 30287802]
32. Summers P, Staempfli P, Jaermann T, Kwiecinski S, Kollias S: A preliminary study of the effects of trigger timing on diffusion tensor imaging of the human spinal cord. AJNR Am J Neuroradiol 27:1952–1961, 2006 [PubMed: 17032874]
33. Symms M, Wheeler-Kingshott C, Parker G, Barker G: Zonally-magnified oblique multislice (ZOOM) EPI, in Proceedings of the 8th Meeting of the International Society for Magnetic Resonance in Medicine. Concord, CA: ISMRM, 2000, p 160
34. Sze G, Bravo S, Baierl P, Shimkin PM: Developing spinal column: gadolinium-enhanced MR imaging. Radiology 180:497–502, 1991 [PubMed: 2068319]
35. Tartaglino LM, Flanders AE, Vinitski S, Friedman DP: Metallic artifacts on MR images of the postoperative spine: reduction with fast spin-echo techniques. Radiology 190:565–569, 1994 [PubMed: 8284417]
36. Vargas MI, Delavelle J, Jlassi H, Rilliet B, Viallon M, Becker CD, et al. : Clinical applications of diffusion tensor tractography of the spinal cord. Neuroradiology 50:25–29, 2008 [PubMed: 17909776]
37. Wheeler-Kingshott CA, Hickman SJ, Parker GJ, Ciccarelli O, Symms MR, Miller DH, et al. : Investigating cervical spinal cord structure using axial diffusion tensor imaging. Neuro-image 16:93–102, 2002 [PubMed: 11969321]
38. Wheeler-Kingshott CA, Parker GJ, Symms MR, Hickman SJ, Tofts PS, Miller DH, et al. : ADC mapping of the human optic nerve: increased resolution, coverage, and reliability with CSF-suppressed ZOOM-EPI. Magn Reson Med 47:24–31, 2002 [PubMed: 11754439]
39. Wheeler-Kingshott CA, Trip SA, Symms MR, Parker GJ, Barker GJ, Miller DH: In vivo diffusion tensor imaging of the human optic nerve: pilot study in normal controls. Magn Reson Med 56:446–451, 2006 [PubMed: 16791864]
40. Wilm BJ, Svensson J, Henning A, Pruessmann KP, Boesiger P, Kollias SS: Reduced field-of-view MRI using outer volume suppression for spinal cord diffusion imaging. Magn Reson Med 57:625–630, 2007 [PubMed: 17326167]
41. Xu D, Mori S, Solaiyappan M, van Zijl PC, Davatzikos C: A framework for callosal fiber distribution analysis. Neuroimage 17:1131–1143, 2002 [PubMed: 12414255]
42. Xue Y, Hauskrecht M: Active learning of classification models with Likert-scale feedback. Proc SIAM Int Conf Data Min 2017:28–35, 2017 [PubMed: 28979827]

43. Yeom KW, Holdsworth SJ, Van AT, Iv M, Skare S, Lober RM, et al. : Comparison of readout-segmented echo-planar imaging (EPI) and single-shot EPI in clinical application of diffusion-weighted imaging of the pediatric brain. AJR Am J Roentgenol 200:W437–43, 2013 [PubMed: 23617511]

44. Zhang L: Convergence and stability of the exponential Euler method for semi-linear stochastic delay differential equations. J Inequal Appl 2017:249, 2017 [PubMed: 29070932]

45. Zhang YD, Zhu FP, Xu X, Wang Q, Wu CJ, Liu XS, et al. : Classifying CT/MR findings in patients with suspicion of hepatocellular carcinoma: comparison of liver imaging reporting and data system and criteria-free Likert scale reporting models. J Magn Reson Imaging 43:373–383, 2016 [PubMed: 26119393]

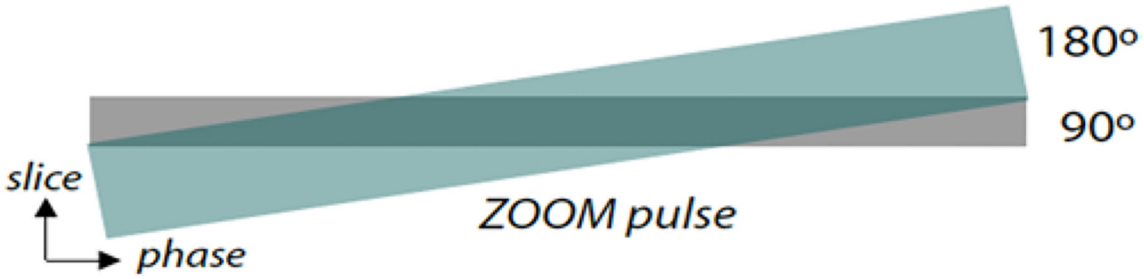

FIG. 1.

The ZOOM-EPI technique,[19,33] which uses a tilted refocusing pulse followed by a 90° slice selective pulse, and a 180° pulse applied obliquely. The resulting parallelogram (*shaded dark green area*) of excited tissue corresponds to the desired rectangular volume.

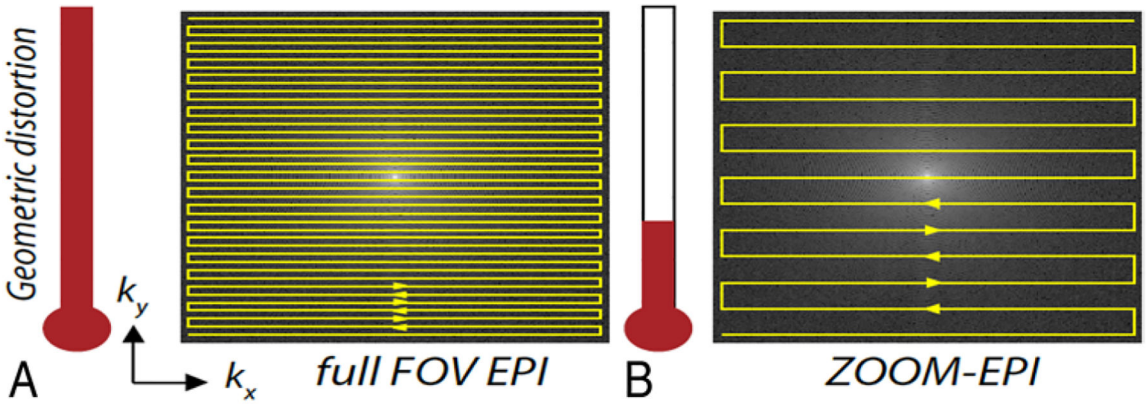

FIG. 2.

Reduction of distortion as one moves from a full FOV EPI (**A**) to a rectangular FOV with ZOOM-EPI (**B**). For the parameters used in this work, this "distortion meter" accompanying the trajectories is drawn to scale. k_x *and* k_y refer to the x (horizontal) and y (vertical) axes of *k*-space, an abstract concept for the image space storing raw data obtained by MRI before mathematical processing.

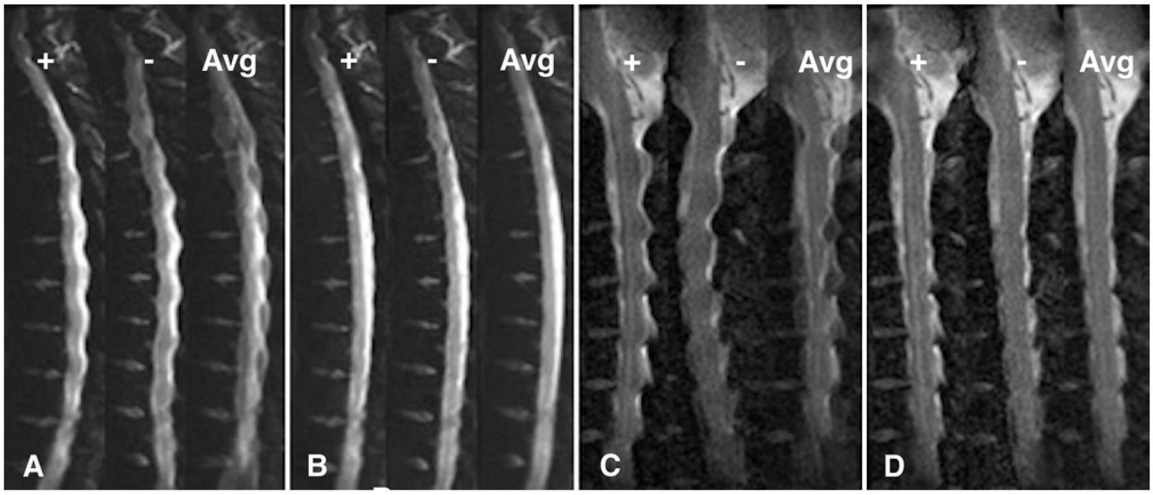

FIG. 3.

Thoracic and cervical $b = 0$ images demonstrating positive distortion (+), negative distortion (−), and the average of both directions of distortion (Avg). **A and C:** $b = 0$ images where no distortion correction has been applied. **B and D:** The same images after performing distortion correction with the displacement field calculated from the positive (+) and negative (−) images.

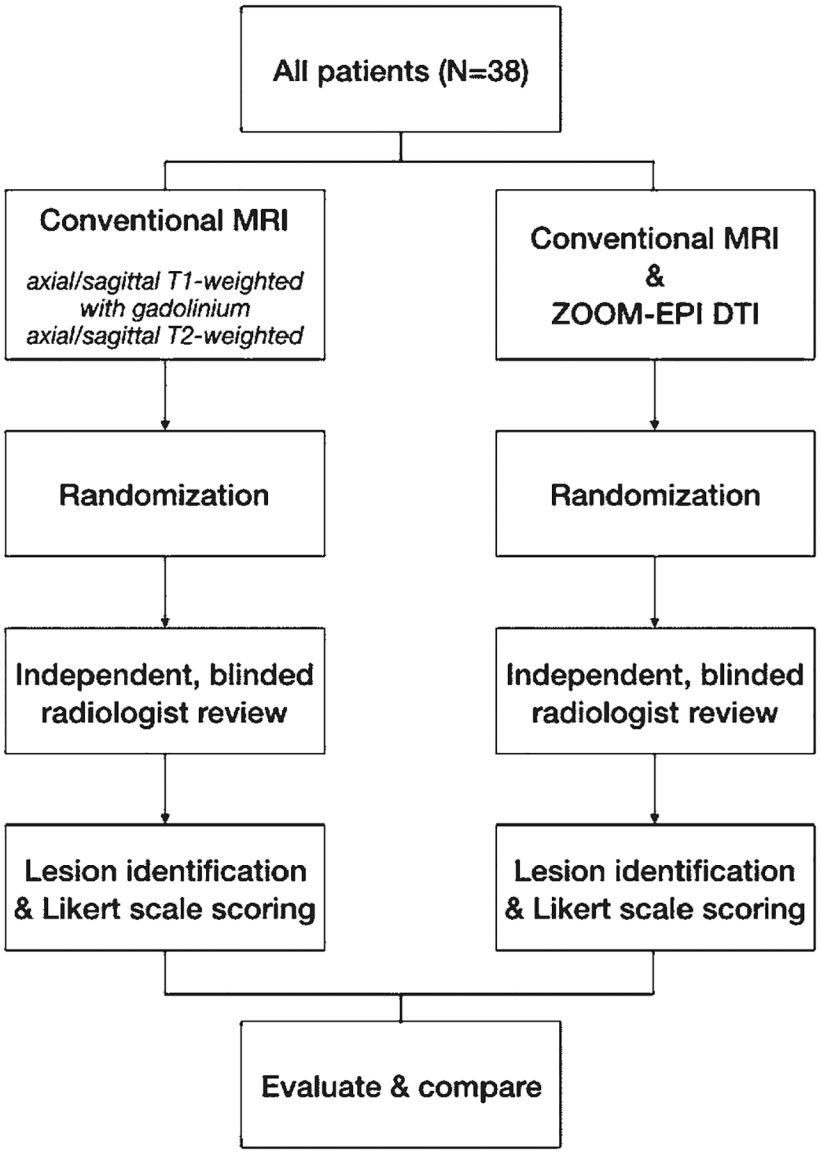

FIG. 4.
Flowchart illustrating the image acquisition and evaluation process.

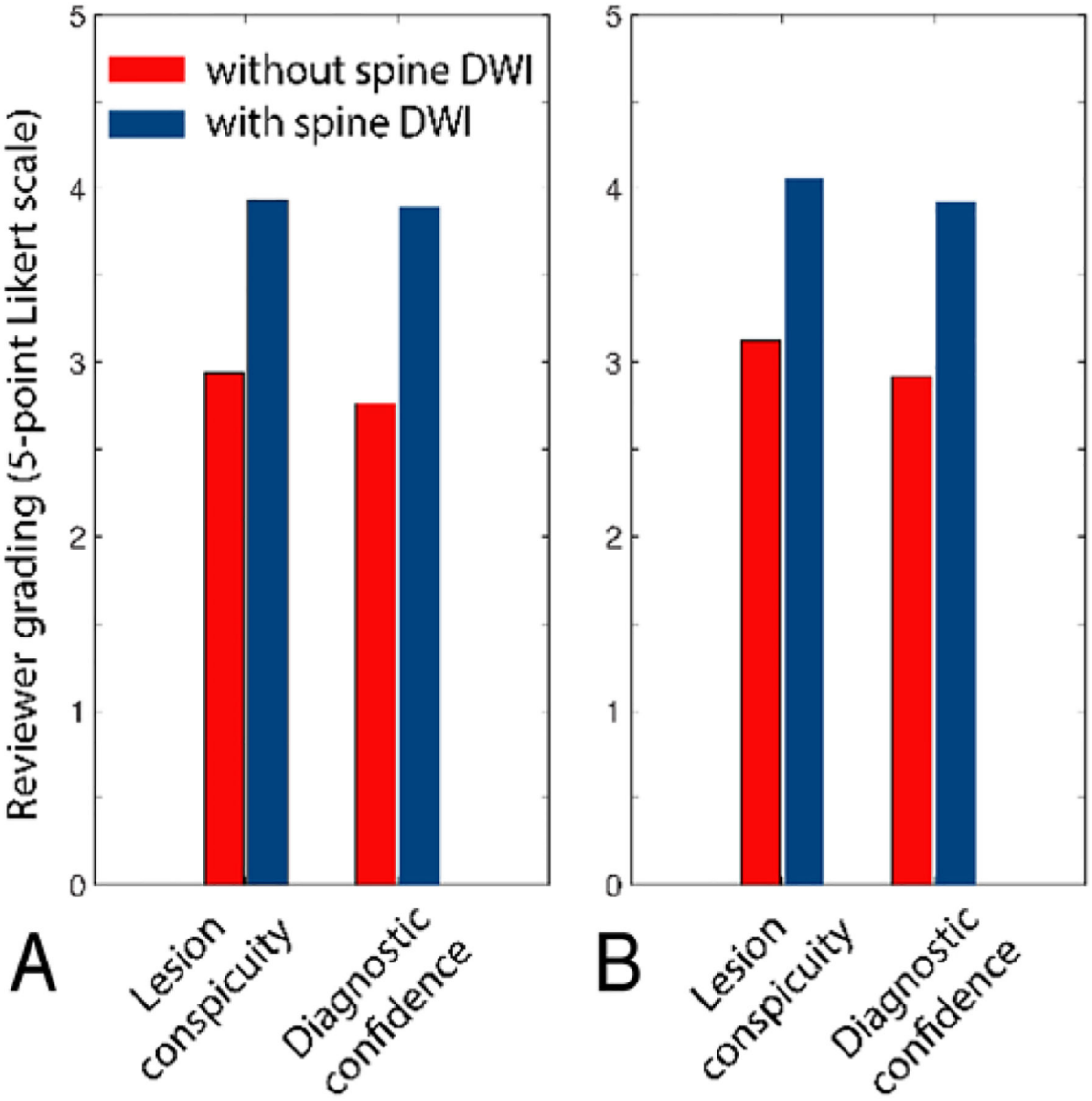

FIG. 5.

Average reviewer grades as measured by Likert scale scores from MR images obtained in 38 patients with or without the addition of performed ZOOM-EPI DTI of the spine, read by the first reviewer (**A**) and the second reviewer (**B**).

FIG. 6.

Images obtained in a 6-year-old girl with a brainstem pilocytic astrocytoma. Sagittal contrast-enhanced T1-weighted image (**A**), sagittal diffusion-weighted image (**B**), sagittal ADC (**C**), sagittal FA (**D**), and sagittal colored FA map (**E**). Note the position of the fourth ventricle relative to mass.

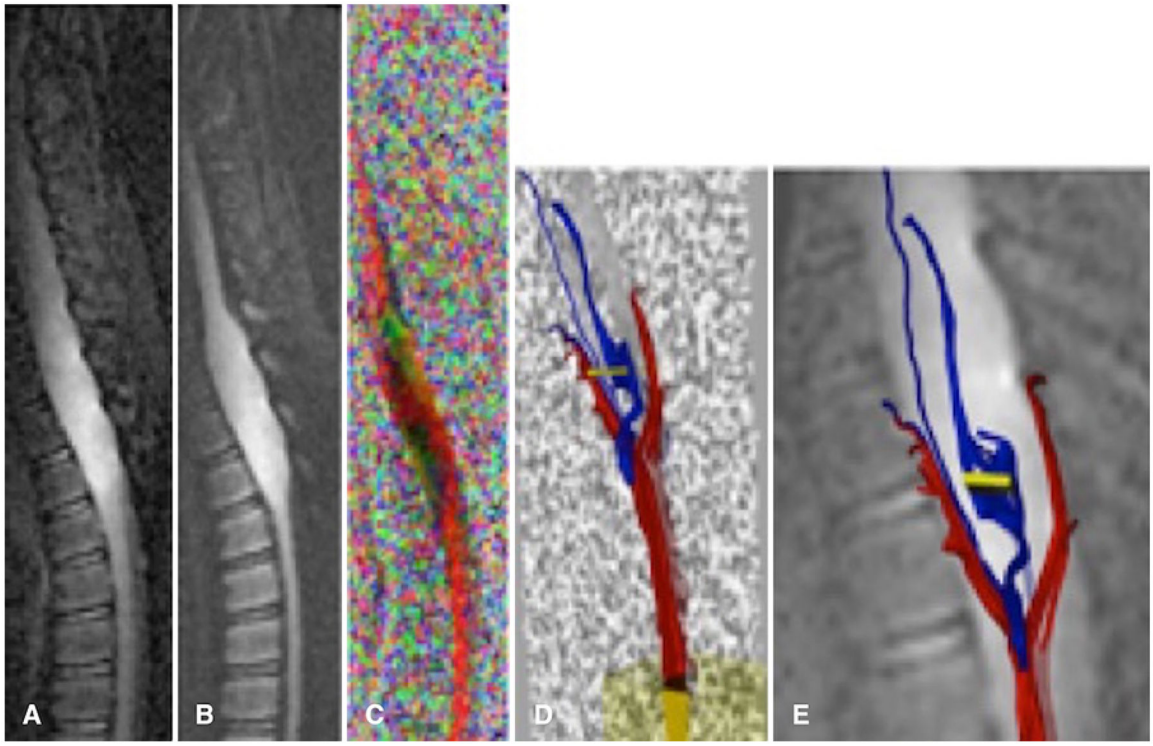

FIG. 7.

Images obtained in a 5-year-old boy with infiltrating grade II astrocytoma. Sagittal $b = 0$ (**A**), iso-diffusion-weighted image (**B**), color FA (**C**), and tractography (**D and E**). Note the tract profiles traversing within this infiltrating spinal cord tumor.

TABLE 1.

Demographic and clinical characteristics of the study cohort

Variable	Value
No. of patients	38
Mean age, yrs	8.0 ± 7.2
Sex	
Female	26 (68.4)
Male	12 (31.6)
Lesion pathology	
Ependymoma	3 (7.9)
Pilocytic astrocytoma	5 (13.2)
Pilomyxoid astrocytoma	1 (2.6)
Diffuse astrocytoma	1 (2.6)
Glioblastoma	1 (2.6)
Medulloblastoma	9 (23.7)
Schwannoma	2 (5.3)
Ganglioglioma	2 (5.3)
ATRT	2 (5.3)
Germinoma	2 (5.3)
PNET	2 (5.3)
Neuroblastoma	2 (5.3)
Other*	6 (15.8)
Primary site of disease	
Cerebrum	4 (10.5)
Posterior fossa	14 (36.8)
Spine vertebrae	3 (7.9)
Spinal cord	12 (31.6)
Other†	5 (13.2)

ATRT = atypical teratoid rhabdoid tumor; PNET = primitive neuroectodermal tumor.

Values are expressed as mean ± standard deviation or number of patients (%).

*Other lesion pathologies include optic pathway glioma, neuroblastoma, neurocutaneous melanosis, choroid plexus carcinoma, meningioma, pineoblastoma, and benign lymphovascular lesion.

†Other sites include optic chasm, lateral ventricle, pituitary stalk, and pineal gland.